iScience

CellPress
OPEN ACCESS

Article

Identification of XD23 as a potent inhibitor of osteosarcoma via downregulation of DKK1 and activation of the WNT/β-catenin pathway

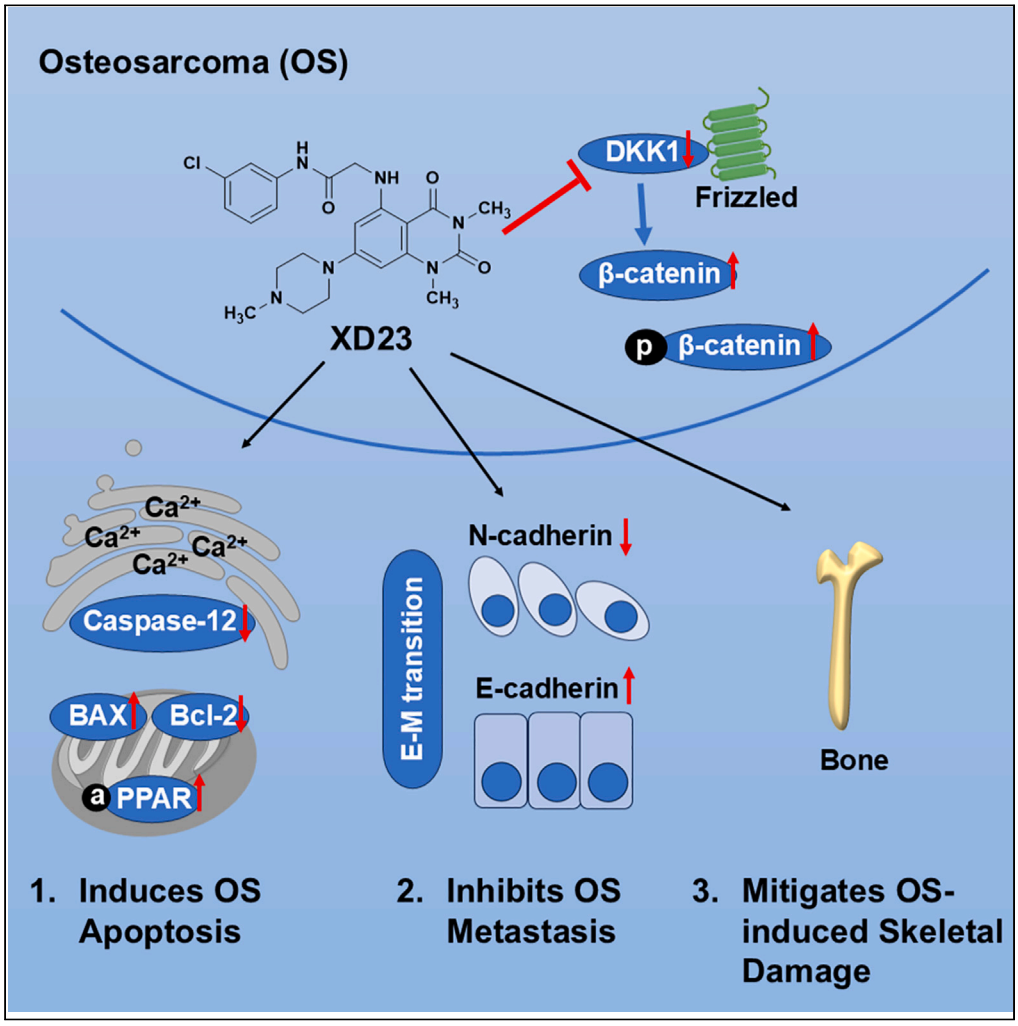

Qian Xie, Yanni Shen, Yipei Yang, ..., Chun Hu, Yan Wang, Huiren Tao

xqqx1996@163.com (Q.X.)
yan.wang@siat.ac.cn (Y.W.)
huiren_tao@163.com (H.T.)

Highlights

XD23 effectively inhibits osteosarcoma proliferation, metastasis, and bone destruction

XD23 reduces DKK1 expression, activating the WNT-β/Catenin pathway

The study confirms the role of DKK1 in osteosarcoma development

Findings support DKK1 inhibitors as new therapies for osteosarcoma

Xie et al., iScience 27, 110758
September 20, 2024
https://doi.org/10.1016/j.isci.2024.110758

iScience

CellPress
OPEN ACCESS

Article

Identification of XD23 as a potent inhibitor of osteosarcoma via downregulation of DKK1 and activation of the WNT/β-catenin pathway

Qian Xie,[1,2,6,*] Yanni Shen,[3] Yipei Yang,[3] Jianhui Liang,[3] Tailin Wu,[1] Chun Hu,[4] Yan Wang,[3,*] and Huiren Tao[5,*]

SUMMARY

Osteosarcoma, the most prevalent malignant bone tumor, is notorious for its aggressive growth and invasiveness. The highly mutable genome of osteosarcoma has made identifying a key oncogene challenging, hindering the development of targeted treatments. Our study validates the effectiveness of XD23, an anti-cancer agent we previously identified, in curbing osteosarcoma proliferation, metastasis, EMT differentiation, and bone destruction and promoting osteosarcoma apoptosis. It further elucidated that XD23 thwarts osteosarcoma by suppressing DKK1 expression, which in turn activates the WNT-β/Catenin pathway. This research presents the concrete evidence of DKK1's involvement in osteosarcoma development, offering a foundation for the development of DKK1 inhibitors as novel treatments for this disease.

INTRODUCTION

Osteosarcoma (OS) is a malignant bone tumor predominantly affecting children and adolescents.[1] The established treatment protocol for OS includes neoadjuvant chemotherapy, surgical resection, and adjuvant chemotherapy.[2] Regrettably, about 85% of OS cases are diagnosed at the metastatic stage, often in the lungs, resulting in a dismal five-year survival rate below 25%.[3] First-line chemotherapy treatments for metastatic OS comprise high-dose methotrexate, cisplatin, doxorubicin, and ifosfamide, used either sequentially or in combination.[4–6] Nonetheless, these medications carry substantial toxicity and often lead to resistance. Alternative chemotherapeutic agents like pamidronate have been tested but with disappointing outcomes.[7] The genomic instability of OS, its varied subtypes, and the lack of clearly defined targets have obstructed the progress of targeted drug therapies.[8,9] The stagnation in developing new treatments for metastatic OS over the last thirty years has stalled clinical advancements, underlining the critical need for more effective, targeted therapies.

Dickkopf-related protein 1 (DKK-1) is a glycoprotein mainly secreted by osteoblasts and bone cells.[10,11] It belongs to the Dickkopf family and functions as an endogenous inhibitor of the canonical Wnt/β-catenin signaling pathway.[12] DKK1 interrupts this pathway by competitively inhibiting the binding of Wnt to Frizzled-related proteins and by binding to LRP5/6 receptors and Kremen1/2 co-receptors, triggering their internalization.[13] This inhibition is crucial in regulating tumor cell proliferation, differentiation, invasion, apoptosis, and metastasis.[14–16] Promising clinical and preclinical results have been observed with several DKK1 inhibitors, such as DKN-01,[17] BHQ-880,[18] JS015,[19] and IIIC3,[20] in treating advanced solid tumors. High DKK1 expression levels in bone malignancies like multiple myeloma[21] and metastatic bone tumors can disrupt bone formation and encourage resorption, leading to bone degradation.[22] However, the role of DKK1 in OS remains uncertain.[23] Some studies proposed that it functions as an oncogene,[24,25] while others argued that it acts as an OS suppressor gene.[26] There is still no definitive evidence of DKK1's effects on OS cell proliferation, differentiation, migration, or its impact on bone integrity.

Given the significant involvement of DKK1 and the Wnt/β-catenin signaling pathway in bone-destructive diseases, it is reasonable to hypothesize that DKK1 may act as an oncogene in OS. However, more research is necessary to clarify DKK1's precise function in OS and its viability as a treatment target. XD23, a small molecule compound designed and synthesized by our laboratory, and it has demonstrated broad-spectrum antitumor activity, as highlighted in our published research.[27] In this study, we aim to evaluate the effectiveness of XD23 in inhibiting metastatic OS by targeting DKK1 and activating the WNT/β-catenin signaling pathway. Through extensive pharmacological experiments conducted at the genetic, cellular, and animal levels, we aim to provide compelling evidence supporting the use of DKK1 small molecule inhibitors as a promising treatment option for metastatic OS.

[1]Department of Orthopedics, Shenzhen University General Hospital, Shenzhen 518055, China
[2]Guangdong Key Laboratory for Biomedical Measurements and Ultrasound Imaging, National-Regional Key Technology Engineering Laboratory for Medical Ultrasound, School of Biomedical Engineering, Shenzhen University Medical School, Shenzhen 518060, China
[3]Center for Translational Medicine Research and Development, Shenzhen Institute of Advanced Technology, Chinese Academy of Sciences, Shenzhen 518055, China
[4]Key Laboratory of Structure-based Drug Design & Discovery, Ministry of Education, School of Pharmaceutical Engineering, Shenyang Pharmaceutical University, Shenyang 110016, China
[5]Department of Orthopaedics and Traumatology, The University of Hong Kong-Shenzhen Hospital, Shenzhen 518053, China
[6]Lead contact
*Correspondence: xqqx1996@163.com (Q.X.), yan.wang@siat.ac.cn (Y.W.), huiren_tao@163.com (H.T.)
https://doi.org/10.1016/j.isci.2024.110758

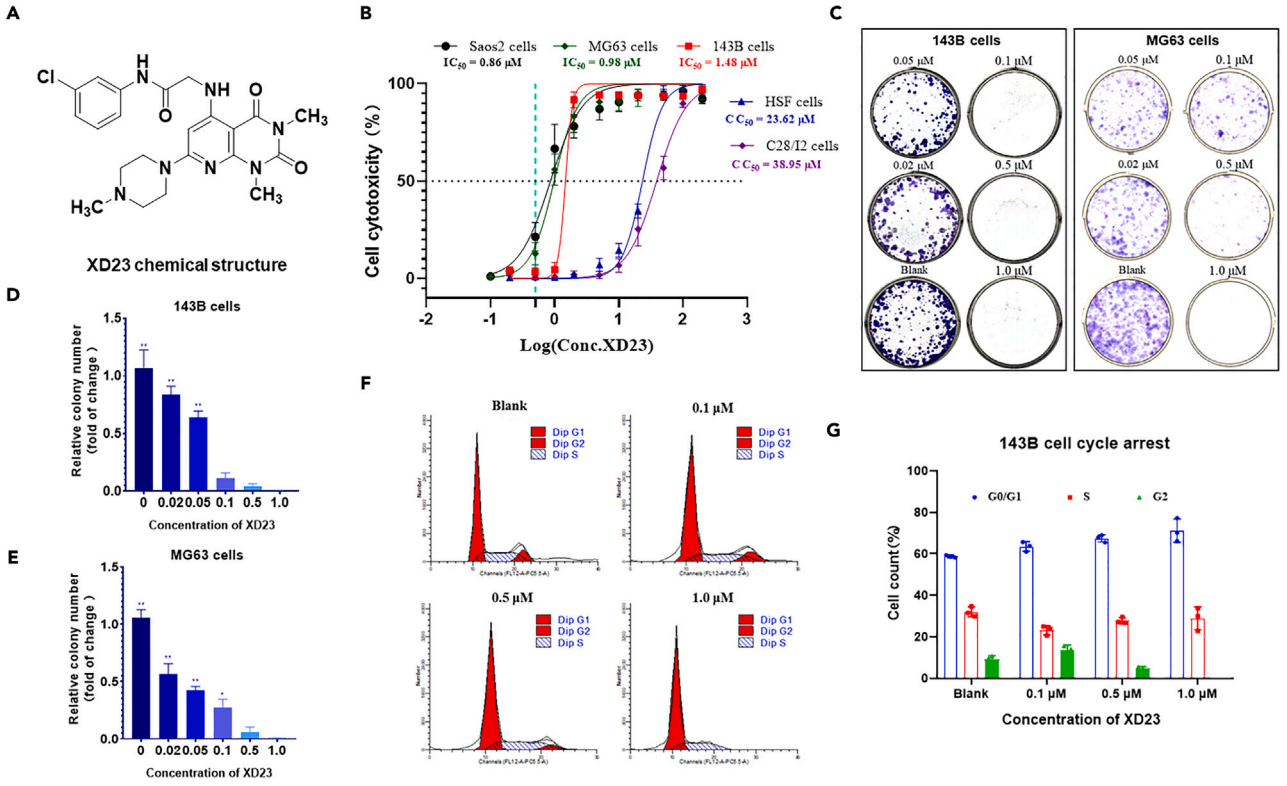

Figure 1. XD23's *in vitro* effects on OS cell proliferation and G0/G1 phase arrest

(A) XD23's chemical structure; (B) IC_{50} values for OS cell lines and CC50 for normal cells post XD23 treatment.

(C–E) Plate colony formation effects of XD23 and quantitative results in 143B (D) and MG63 cells (E).

(F and G) Flow cytometry analysis of the cell cycle in OS cells and quantitative outcomes. *$p < 0.05$; **$p < 0.01$. Data was analyzed by one sample t-test.

RESULTS

XD23 suppresses cell proliferation and induces G0/G1 phase arrest in OS cells

In our lab, we synthesized a series of pyridine[2,3-*d*]pyrimidine compounds,[26,27] with XD23 (Mol. Wt. = 471.18 g/mol, cLogP = 3.47, Figure 1A) emerging as the most effective against OS. We assessed the anti-proliferative effects of XD23 on three human OS cell lines—Saos2, MG63, and 143B—using CCK-8 assays, which showed IC_{50} values at 48h of 0.86 μM, 0.98 μM, and 1.48 μM, respectively. For comparison, normal human cell lines C28/I2 and HSF demonstrated CC_{50} values at 48h of 38.95 μM and 23.62 μM, respectively. This indicates a 16 to 45-fold selectivity for targeting cancer cells. At 0.5 μM, XD23 shows no cytotoxicity toward normal cells but inhibits the proliferation of three osteosarcoma cell lines by 5%–30%. Concentrations slightly above 0.5 μM exceed the IC_{50}, while those slightly below have minimal effect. Hence, 0.5 μM XD23 was selected for further mechanistic studies (Figure 1B). Additionally, XD23's ability to significantly reduce colony formation in OS cells further confirms its suppressive role in cell proliferation (Figures 1C–1E). Flow cytometry analysis showed a significant rise in the percentage of OS cells in the G0/G1 phase, suggesting that XD23 induces G0/G1 arrest (Figures 1F and 1G). Overall, the data robustly supports XD23's capability to halt OS cell growth and trigger G0/G1 phase arrest.

XD23 induces apoptosis in OS cells via mitochondrial and ER pathway

Next, the potential of XD23 to induce apoptosis in OS cells were probed. After 24 h of exposure to 0.5 μM XD23, mitochondrial permeability transition pores were compromised in two OS cell lines, indicated by a marked decrease in orange mitochondrial fluorescence (Figure 2A). Flow cytometry analysis revealed a dose-dependent increase in the number of early and late apoptotic cells in OS cells treated with XD23, with the percentages escalating from 3.52% to 10.8% and 1.21–29.1% respectively (Figures 2B and 2C). This data reinforces the pro-apoptotic effect of XD23.

The apoptotic mechanism was further confirmed by increased caspase-3 activation, a key apoptosis regulator,[28] in 143B and MG63 cells with ascending XD23 doses. PARP cleavage, which prompts caspase-3 to induce apoptosis,[29] was observed in 143B cells but not in MG63 cells. XD23 also disrupted the Bcl-2 family protein balance by elevating the ratio of pro-apoptotic protein BAX to anti-apoptotic protein Bcl-2 in OS cells, thereby favoring apoptosis (Figures 2D–2F). These findings collectively suggest that XD23 initiates apoptosis in OS cells predominantly through the mitochondrial pathway.

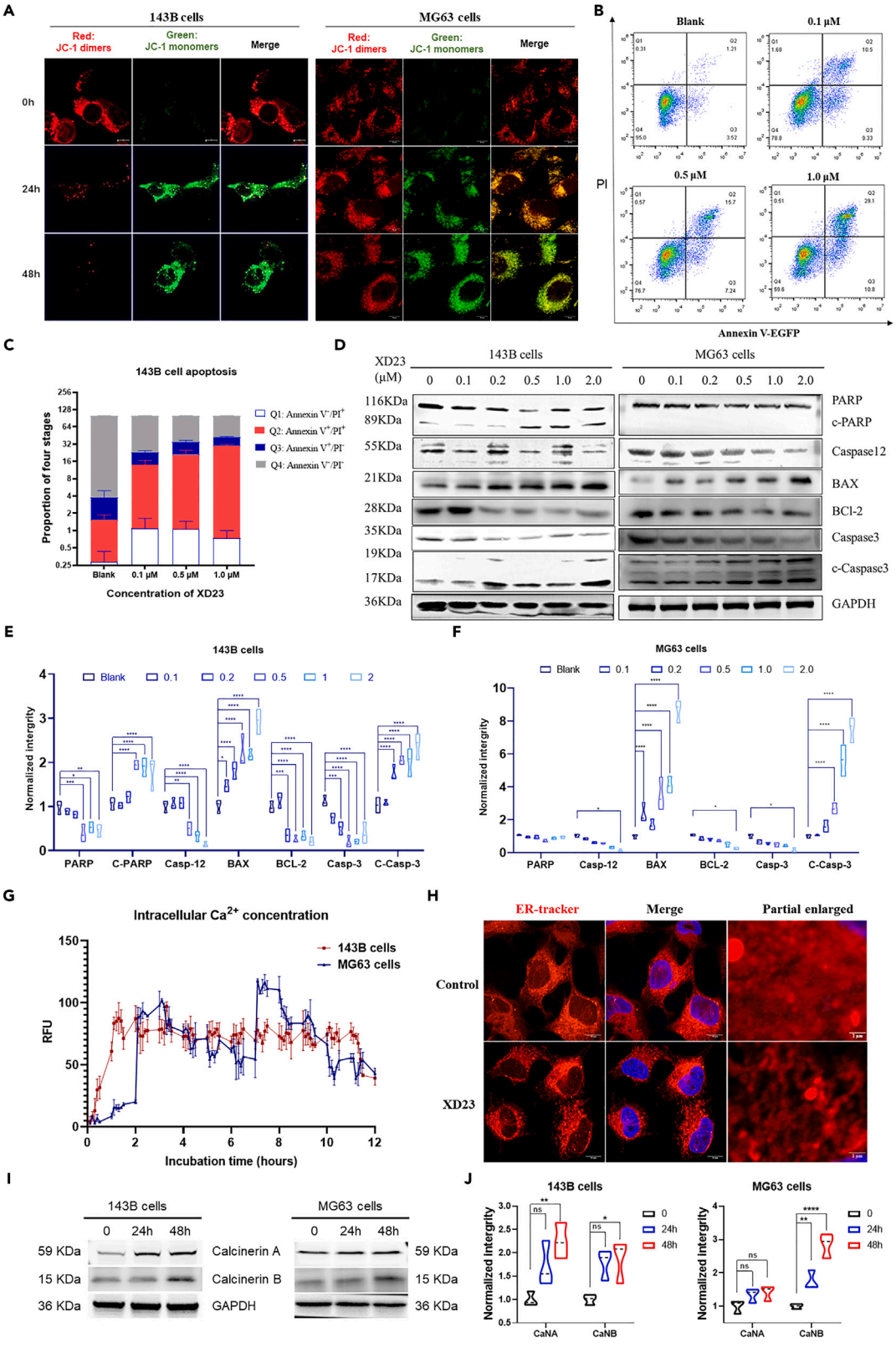
A
143B cells
MG63 cells
Red: JC-1 dimers
Green: JC-1 monomers
Merge
0h
24h
48h
B
Blank
0.1 μM
0.5 μM
1.0 μM
PI
Annexin V-EGFP
C
143B cell apoptosis
Proportion of four stages
Q1: Annexin V-/PI+
Q2: Annexin V+/PI+
Q3: Annexin V+/PI-
Q4: Annexin V-/PI-
Blank
0.1 μM
0.5 μM
1.0 μM
Concentration of XD23
D
XD23 (μM)
143B cells
MG63 cells
0 0.1 0.2 0.5 1.0 2.0
116KDa
89KDa
55KDa
21KDa
28KDa
35KDa
19KDa
17KDa
36KDa
PARP
c-PARP
Caspase12
BAX
BCl-2
Caspase3
c-Caspase3
GAPDH
E
143B cells
Blank 0.1 0.2 0.5 1 2
Normalized intergrity
PARP
C-PARP
Casp-12
BAX
BCL-2
Casp-3
C-Casp-3
F
MG63 cells
Blank 0.1 0.2 0.5 1.0 2.0
Normalized intergrity
PARP
Casp-12
BAX
BCL-2
Casp-3
C-Casp-3
G
Intracellular Ca2+ concentration
143B cells
MG63 cells
RFU
Incubation time (hours)
H
ER-tracker
Merge
Partial enlarged
Control
XD23
I
143B cells
MG63 cells
0 24h 48h
59 KDa
15 KDa
36 KDa
Calcinerin A
Calcinerin B
GAPDH
J
143B cells
MG63 cells
Normalized Intergrity
0
24h
48h
CaNA
CaNB

Figure 2. XD23 promotes apoptosis in OS cells by elevating ER Ca^{2+} level

(A) Mitochondrial membrane potential assay with JC-1 staining in OS cells post XD23 treatment for 24h or 48h. Scale bars = 10 μM.

(B and C) Annexin V-FITC/PI-stained OS cells analyzed by flow cytometry.

(D–F) Dose-dependent protein expression changes related to apoptosis in OS cells via western blotting. Normalized protein expression of WB in 143B cells (E) and MG63 cells (F).

(G) Fluro-4 AM detection of Ca^{2+} dynamics in OS cells treated with XD23 in 12h.

(H) ER staining in 143B cells treated with XD23. Scale bars = 10 μM.

(I) Western blotting of Calcinerin A and Calcinerin B protein expression after treated with XD23 for 24h or 48h.

(J) Normalized protein expression analysis of (I). *p < 0.05; ** <0.01; ***p < 0.001. Data was analyzed by one-way ANOVA followed by Tukey's multiple comparisons test.

Interestingly, we noted that XD23 stimulation activates caspase-12, an apoptosis-related protein uniquely present on the endoplasmic reticulum (ER),[30] in both 143B and MG63 cells (Figures 2D–2F), implying that the ER pathway also contributes to apoptosis. The activation is further supported by the significant release of calcium ions from the ER calcium pump upon XD23 stimulation. As depicted in Figures 2G and S1, this stimulation escalates the intracellular calcium ion concentration in 143B and MG63 cells.

To confirm that XD23 induces apoptosis in OS cells via the ER stress pathway, we first noted structural changes in the ER using an ER fluorescent probe (Figures 2H and S2). Additionally, we observed a significant upregulation in both the A and B subunits of Calcineurin (Figures 2I and 2J), a protein that responds to calcium ion concentration and indicates ERS activation.[31,32] These findings suggest that XD23 can induce ER stress and promote apoptosis in OS cells by elevating calcium ion concentration.

XD23 attenuates OS cells migration by suppressing EMT differentiation

Extensive research has highlighted a direct link between the overexpression of EMT-related transcription factors in OS and the enhanced migratory and invasive capabilities of OS cells, ultimately driving metastasis. Our transwell migration assay results demonstrate that 0.1 μM XD23 significantly reduces OS cell migration (Figure 3A). Furthermore, a wound healing assay revealed that treating 143B cells with 0.5 μM XD23 for 6 h led to a notable 34% reduction in wound closure, indicating a potent suppression of OS cell invasion by XD23 (Figures 3B and 3C).

Further investigation into the mechanism revealed that XD23 affects the transcriptional control of EMT-related genes in OS cells (Figures 3D and 3E). Our findings showed that post 48 h of stimulation with 0.5 μM XD23, there was a remarkable 8- to 16-fold increase in the expression of the EMT marker gene *E-cadherin*, while *N-cadherin* expression significantly dipped by 3- to 5-fold. Nevertheless, the expression of *Vimentin*, *TJP-1*, or *Snail1* genes remained unaffected. These observations were further corroborated by Western blot (Figures 3F and 3G) and immunofluorescence experiments (Figure 3H), confirming that XD23 indeed upregulates E-cadherin expression and downregulates N-cadherin protein levels. In summary, our experimental data compellingly suggest that XD23 impedes the invasive and migratory tendencies of OS cells by regulating their EMT differentiation.

RNA-seq discloses XD23 inhibits OS by inhibiting DKK1 to activate Wnt/β-catenin signaling pathway

To unravel the mechanism behind XD23's impact on OS cell functions, including proliferation, apoptosis, migration, and differentiation, we performed RNA sequencing on total RNA from 143B cells treated with 0.5 μM XD23 for 48 h. The resulting volcano plot highlighted significant transcriptomic shifts, with 243 genes upregulated and 329 genes downregulated, notably including a pronounced decrease in DKK1 (Figure 4A). Gene Ontology (GO) analysis further implicated XD23 in modulating various tumor-associated pathways, with a particular emphasis on alterations in calcium and Wnt signaling pathways (Figure 4B). Heatmap analysis of gene expression linked to the DKK1-Wnt axis confirmed an induction of Wnt/β-catenin signaling-related genes following DKK1 suppression (Figures 4C and 4D). Additionally, genes interacting with DKK1, such as Wnt5A/B and FZD5/6, and those involved in the Wnt-Ca^{2+} pathway, showed increased expression, a finding substantiated by qPCR results (Figure 4E).

Western blot analysis showed that XD23 reduces DKK1 protein levels and increases β-catenin and its phosphorylated form at 0.2 μM and 0.5 μM concentrations (Figures 4F–4H), indicating that XD23 activates the Wnt/β-catenin pathway by inhibiting DKK1 *in vitro*. To explore the role of DKK1 in XD23's anti-OS activity, *Dkk1* transfected overexpressing 143B cells were generated (Figure 4I). These cells showed high DKK1 protein levels with reduced β-catenin, which normalized after XD23 treatment, resembling wild-type 143B cells (Figures 4I and 4J). Comparing the growth-inhibitory effects of XD23 on *Dkk1*-overexpressing cells to wild-type revealed a 2.9-fold decrease in efficacy for the former, underscoring DKK1's significance in XD23's mechanism (Figure 4K). In conclusion, our findings strongly indicate that XD23's anti-OS activity *in vitro* is due to a pharmacological mechanism that involves Wnt/β-catenin pathway activation through DKK1 inhibition.

XD23 suppresses orthotopic OS tumor growth and metastasis *in vivo*

In our investigation of XD23's efficacy against metastatic OS, we developed an orthotopic mouse model by inoculating rat-derived OS cells (UMR-106) into the distal tibia bone marrow. Commencing one-week post-inoculation, XD23 was administered orally at 15 mg/kg and 10 mg/kg for high and low doses, respectively, 2–3 times weekly over a four-week period As a control, we used high-dose methotrexate (MTX) at 10 mg/kg, with a 5 mg/kg folic acid supplement 24 h after MTX administration (Figure 5A).

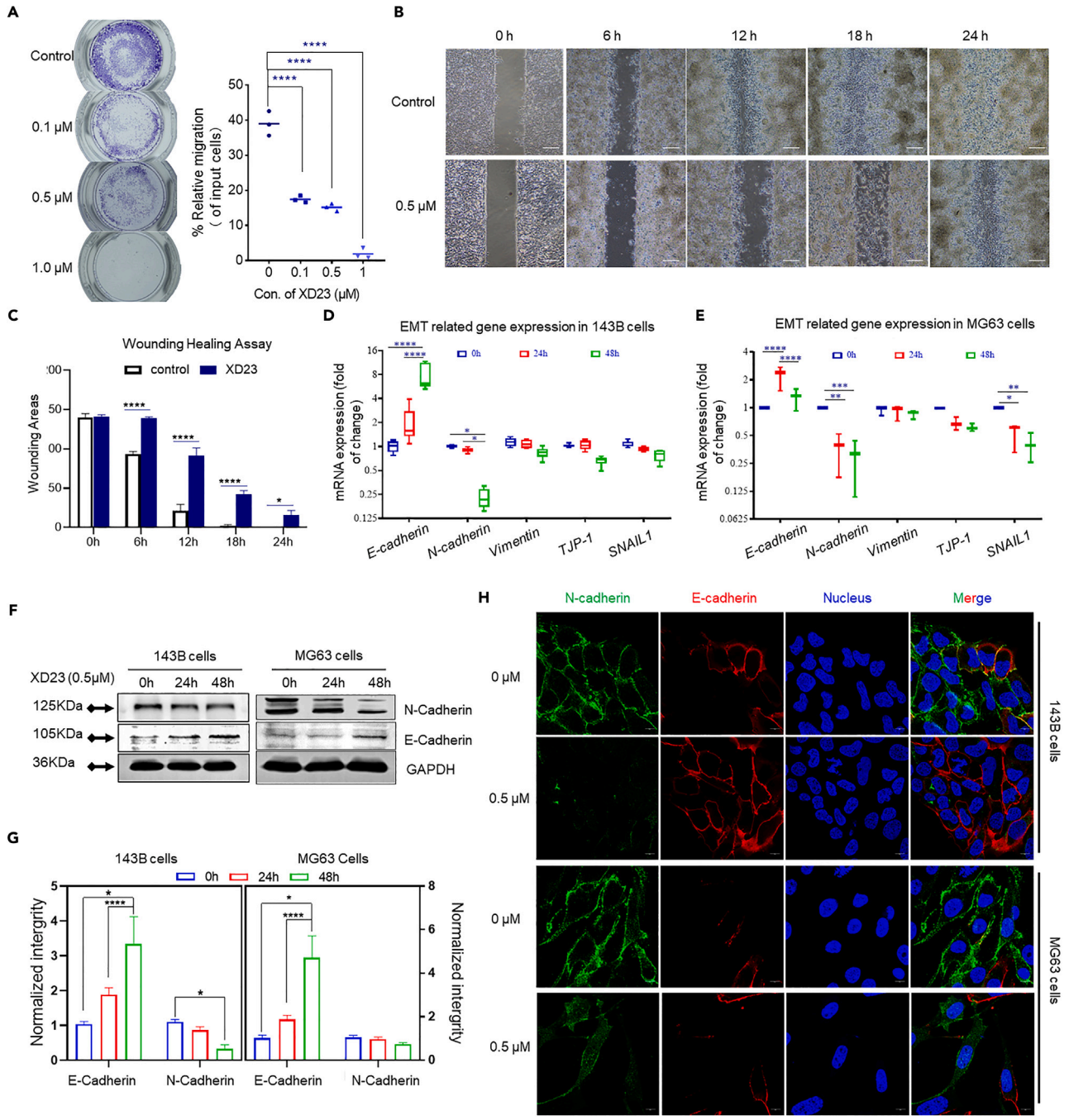

Figure 3. XD23 deters OS cells migration by impeding EMT differentiation

(A) Transwell migration assay showing concentration-dependent inhibition of 143B cell invasion by XD23.

(B) Wound healing assay demonstrating the inhibitory effect of XD23 (0.5 μM) on 143B cell migration and (C and C) the normalized wounding areas. Scale bars = 200 μM.

(D and E) Changes of mRNA expression related to EMT differentiation after XD23 (0.5 μM) stimulation in 143B cells and MG63 cells.

(F) E-cadherin and N-cadherin protein expression after treated with XD23 (0.5 μM) for 24h and 48h.

(G) Normalized expression of E-cadherin and N-cadherin protein expression in western blotting.

(H) Immunofluorescence staining for E-cadherin and N-cadherin in 143B and MG63 cells post-XD23 treatment. Scale bars = 10 μM *$p < 0.05$; **$p < 0.01$; ***$p < 0.001$; ****$p < 0.0001$. Data was analyzed by one-way ANOVA followed by Tukey's multiple comparisons test.

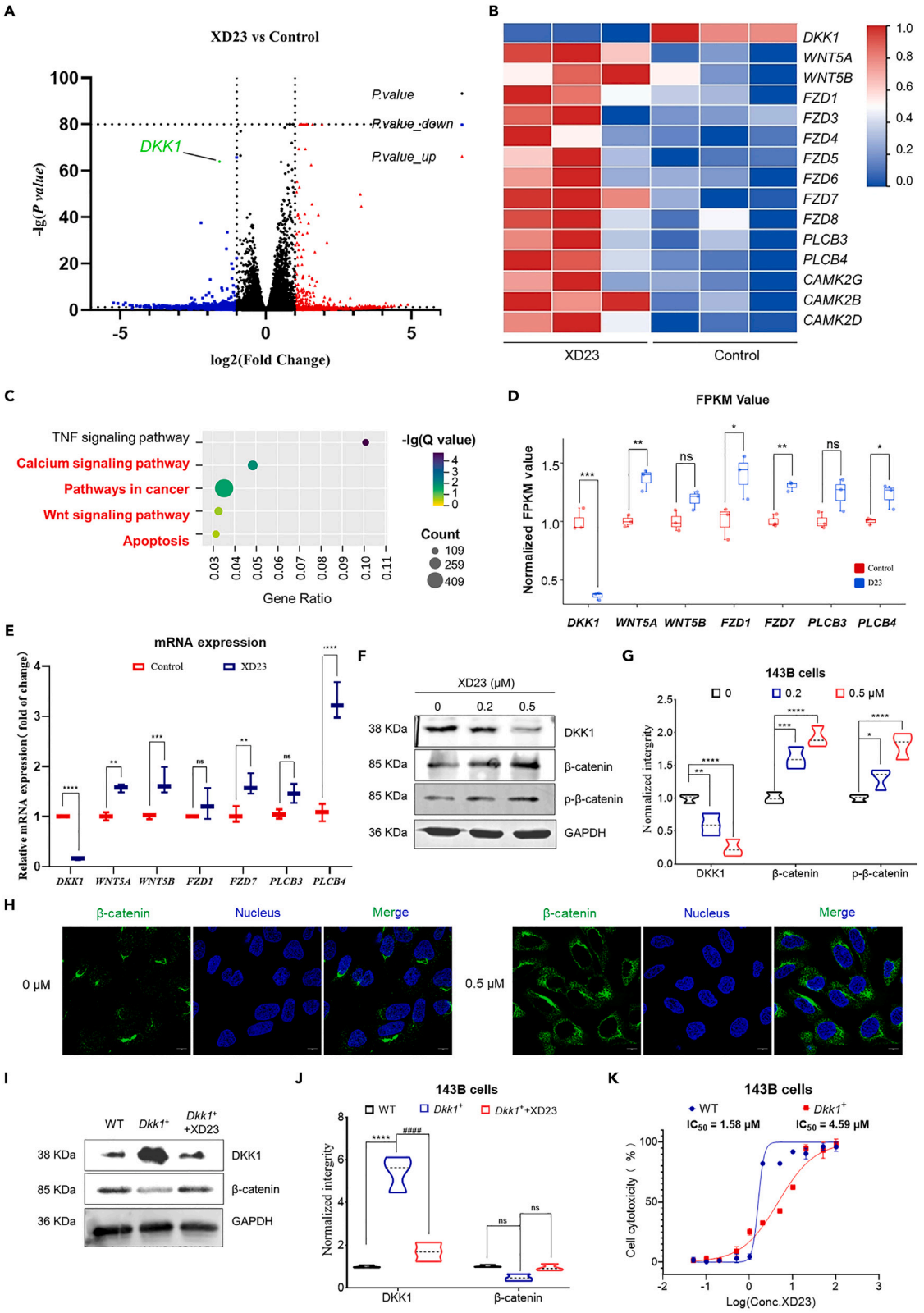
A
XD23 vs Control
P.value
P.value_down
P.value_up
DKK1
-lg(P value)
log2(Fold Change)
B
DKK1
WNT5A
WNT5B
FZD1
FZD3
FZD4
FZD5
FZD6
FZD7
FZD8
PLCB3
PLCB4
CAMK2G
CAMK2B
CAMK2D
XD23
Control
C
TNF signaling pathway
Calcium signaling pathway
Pathways in cancer
Wnt signaling pathway
Apoptosis
-lg(Q value)
Count
Gene Ratio
D
FPKM Value
Normalized FPKM value
Control
D23
E
mRNA expression
Control
XD23
Relative mRNA expression(fold of change)
F
XD23 (μM)
38 KDa
85 KDa
85 KDa
36 KDa
DKK1
β-catenin
p-β-catenin
GAPDH
G
143B cells
Normalized intergrity
H
β-catenin
Nucleus
Merge
0 μM
0.5 μM
I
WT
Dkk1+
Dkk1+ +XD23
38 KDa
85 KDa
36 KDa
DKK1
β-catenin
GAPDH
J
143B cells
Normalized intergrity
K
143B cells
IC50 = 1.58 μM
IC50 = 4.59 μM
Cell cytotoxicity (%)
Log(Conc.XD23)

Figure 4. XD23 inhibits OS by downregulating DKK1 to activate Wnt signaling pathway

(A) The Volcano plot showing gene expression differences between XD23-treated and control groups (n = 3 biologically independent cell samples). Significant genes identified using Cuffdiff, with upregulated transcripts marked in red and downregulated in blue.

(B) GO analysis of biological processes affected by regulated genes.

(C–G) Heatmap of Wnt pathway gene expression changes. Representative gene FPKM values (D) and qPCR validation (E). Western blotting results (F) and the normalized quantitative results (G) of WNT signaling pathway related proteins in 143B cells after XD23 stimulation.

(H–J) The immunofluorescence analysis of β-catenin in 143B cells after treated with XD23. Scale bars = 10 μM. Western blotting results (I) and the normalized quantitative results (J) of overexpression *Dkk1* transfected 143B cells. $^{####}p < 0.0001$ vs. *Dkk1*$^{+}$. $^{****}p < 0.0001$ vs. WT.

(K) Comparison of cell cytotoxicity results of XD23 on WT-type 143B cells and *Dkk1* overexpressing 143B cells. $^{*}p < 0.05$; $^{**}p < 0.01$; $^{***}p < 0.001$; $^{****}p < 0.0001$. ns = no significance. Data was analyzed by one-way ANOVA followed by Tukey's multiple comparisons test.

The Model group, receiving saline, began to show mortality from day 15, with no survivors by the end of the treatment period. The MTX group exhibited mortality beginning on day 19, with a survival rate of 25% at the end of the study. By contrast, the XD23-treated mice demonstrated improved survival, with no deaths until days 23 and 27 for low and high doses, respectively, culminating in a 75% survival rate, a marked enhancement over MTX (Figure 5B). Additionally, body weight changes showed decreased weight in all OS groups compared to the Sham group. Notably, the MTX group experienced a sharp drop in the final week. In contrast, the XD23 groups maintained their body weight more effectively (Figure 5C). Histological analysis with hematoxylin and eosin (H&E) staining of visceral organs showed no discernible organ toxicity from XD23, confirming its safety *in vivo* (Figure S3). The XD23 groups, especially at the higher dose, showed a notable reduction in hindlimb sarcoma volume versus the MTX group, underscoring XD23's potent anti-proliferative effects (Figure 5D). Examinations of the lungs postmortem revealed extensive tumor formation in the control group, signifying advanced pulmonary metastasis. However, gross (Figure S4) and H&E (Figure 5E) inspections of the XD23 groups indicated significantly less metastatic spread compared to the MTX group, highlighting XD23's potential in curbing metastatic progression in OS. Therefore, XD23 has proven to suppress OS proliferation and metastasis *in vivo*, showing promise in limiting the advancement and dissemination of lung metastatic OS. Further studies are needed to confirm if its effects are due to DKK1 inhibition *in vivo*.

XD23 mitigates OS-induced skeletal damage *in vivo*

Micro-CT scans of the right tibia in each mouse group (Figure 5F) revealed severe cortical bone erosion in the OS-affected mice, characterized by thinning bone shafts and visible cavities, bordering on fracture. In contrast, mice treated with MTX demonstrated an appreciable increase in bone mass compared to the model group. Most strikingly, XD23 treatment yielded pronounced cortical bone thickening and structural reinforcement, suggesting a role for the compound in halting OS growth and reducing bone loss. Furthermore, *in vitro* osteoclast culture experiments revealed that high concentrations of XD23 (10μM and 3μM) can significantly inhibit osteoclast differentiation (Figure S5). To encapsulate, these results support XD23's potential as a therapeutic agent in alleviating OS-induced skeletal deterioration.

XD23 curbs orthotopic OS tumor through DKK1 inhibition and WNT/β-catenin signaling pathway activation

Histological examination of H&E-stained tibial tumor sections from each mouse group revealed densely packed cells within a thin fibrous capsule, indicative of OS (Figure 6A). Further staining experiments will be conducted on *in situ* OS and pulmonary metastatic OS samples to confirm if XD23, as hypothesized, also downregulates DKK1 to activate the Wnt/β-catenin signaling pathway *in vivo*, thereby suppressing OS cell proliferation and metastasis, promoting apoptosis, and mitigating bone destruction.

Initial TUNEL assays demonstrated that high-dose XD23 markedly induced apoptosis in OS cells in tumor OS cells, with effectiveness similar to lower doses of MTX (Figures 6B and 6C). Immunohistochemistry of tibial and pulmonary OS samples showed marked DKK1 suppression in the XD23-treated group compared to the Model groups (Figures 6D and 6E), while β-catenin levels were sustained in the Model and high-dose XD23 groups (Figures 6D and 6F). Lung metastases displayed high DKK1 levels, which XD23 significantly reduced compared to MTX. Conversely, β-catenin expression was minimal in the MTX group but increased with high-dose XD23 (Figures 6G–6I). These findings imply that XD23 modulates the Wnt/β-catenin pathway by reducing DKK1 expression, enhancing β-catenin activity, and contributing to bone preservation (Figure 6J).

DISCUSSION

DKK1 is crucial in the Wnt/β-catenin signaling pathway, significantly affecting the onset, progression, and therapeutic response in OS.[33,34] High DKK1 expression correlates with worsened malignancy and prognosis in OS,[23,35] but its over-suppression could inadvertently trigger oncogenic Wnt/β-catenin signaling.[36] Thus, DKK1-targeted therapies must be finely tuned to effectively check tumor growth and dissemination.

This research presents the anticancer agent XD23, which modulates DKK1, thereby influencing Wnt/β-catenin signaling. XD23's antitumor potency correlates with DKK1 expression levels. It curbs proliferation in various OS cell lines, induces cell-cycle arrest, and demonstrates selective toxicity toward OS cells compared to non-cancerous cells. Remarkably, XD23 significantly hampers proliferation in DKK1-overexpressing 143B cells, hinting that its action might also involve additional oncogenic pathways.

Contrary to the norm where aberrant Wnt pathway activation fosters tumor growth and metastasis by blocking apoptosis,[37] this study shows that DKK1 inhibition by XD23 triggers apoptosis in OS cells in a dose-dependent manner. It elevates ER calcium and disrupts

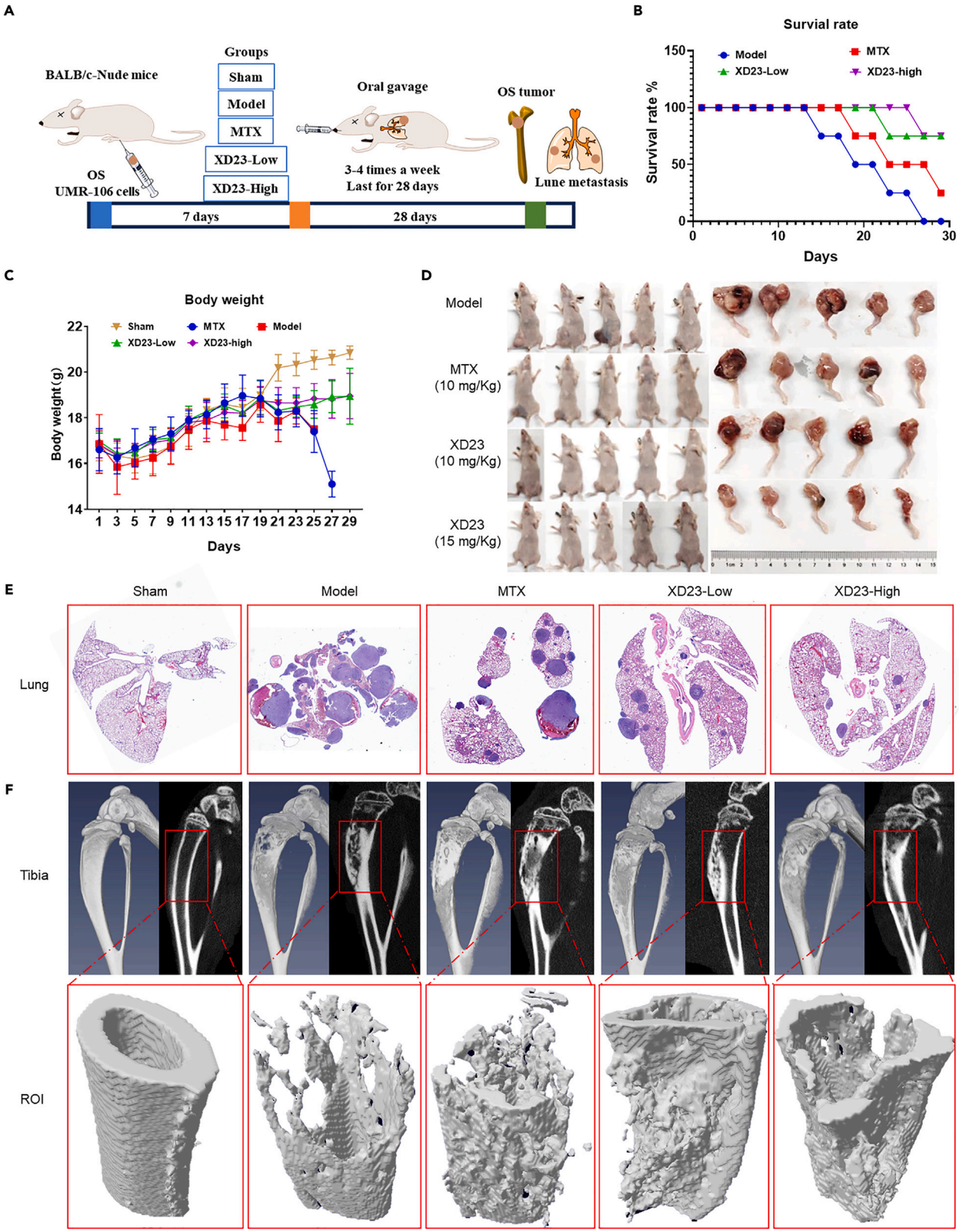
A
BALB/c-Nude mice
Groups
Sham
Model
MTX
XD23-Low
XD23-High
Oral gavage
OS tumor
OS
UMR-106 cells
3-4 times a week
Last for 28 days
Lune metastasis
7 days
28 days
B
Survial rate
Model
MTX
XD23-Low
XD23-high
Survival rate %
Days
C
Body weight
Sham
MTX
Model
XD23-Low
XD23-high
Body weight (g)
Days
D
Model
MTX
(10 mg/Kg)
XD23
(10 mg/Kg)
XD23
(15 mg/Kg)
E
Sham
Model
MTX
XD23-Low
XD23-High
Lung
F
Tibia
ROI

Figure 5. XD23's impact on anti-metastatic OS *in vivo*

(A) Orthotopic metastatic OS mouse model experimental design.
(B) OS mouse survival rates per group.
(C) Mouse body weight fluctuations during the experiment.
(D) Images of OS in the right limb of each mouse group.
(E) Lung H&E staining representations for each group.
(F) Micro-CT scans of each group's right tibia.

mitochondrial membrane potential, suggesting involvement of both mitochondrial and ER pathways. This is the inaugural demonstration of apoptosis promotion through DKK1 inhibition in OS, bolstering the potential of DKK1 antagonists in OS treatment.

Considering the high mortality of OS due to lung metastases,[34] it is vital to understand how Wnt pathway modulation affects OS cell behavior. XD23 effectively hinders OS cell migration, invasion, and epithelial-mesenchymal transition *in vitro* and significantly reduces lung metastasis in OS animal models, indicating that DKK1 inhibition and consequent Wnt/β-catenin pathway activation may impede OS cell metastasis.

The Wnt/β-catenin pathway is indispensable for differentiating bone marrow mesenchymal stem cells into osteoblasts,[38] and its disruption can cause bone diseases like osteoporosis.[39] In advanced OS, bone destruction is a significant hurdle. Our findings indicate that XD23 activates the Wnt/β-catenin pathway via DKK1 inhibition in an *in situ* OS model, unlike methotrexate, potentially conserving bone mass and offering a therapeutic edge in preventing tumor-induced bone loss.

In summary, our investigation validates the antineoplastic properties of XD23, a compound that targets OS by downregulating DKK1 and activating the Wnt/β-catenin pathway. XD23 selectively halts OS cell proliferation, especially in the DKK1-overexpressing 143B cell line. Its antitumor effect is apoptosis-driven, engaging mitochondrial and ER pathways. Moreover, XD23 markedly impedes OS cell migration, invasion, and EMT, contributing to reduced lung metastasis *in vivo*. Divergent from agents like methotrexate, XD23 maintains bone integrity by modulating the Wnt/β-catenin pathway, presenting a benefit in averting tumor-associated bone deterioration. These findings support the clinical investigation of DKK1 inhibitors as a strategy for OS treatment.

Limitations of the study

While this study has systematically investigated the inhibitory mechanism of XD23 on OS, we must acknowledge certain limitations. First, further in-depth research is required to fully understand how XD23 inhibits osteoclast-induced bone resorption. This study has only preliminarily explored its effect on inhibiting osteoclast differentiation, and a more detailed investigation of the mechanisms involved is necessary. Second, although this study has identified the downstream proteins of XD23, there is a need for further exploration of its upstream target proteins. Despite these limitations, the conclusions drawn in this study remain valid. We plan to address these issues in future research to provide more comprehensive evidence supporting the use of XD23 in OS treatment.

RESOURCE AVAILABILITY

Lead contact

Further information and requests for resources and reagents should be directed to and will be fulfilled by the lead contact, Q.X. (xqqx1996@163.com).

Materials availability

The study did not generate new unique reagents.

Data and code availability

- Raw data and processed data were uploaded to Mendeley Data and are available via https://doi.org/10.17632/kb6g5n2nnz.1. RNA-seq raw data were uploaded in the GEO datasets and are available via GSE262143.
- This study did not generate original code.
- Any additional information required to reanalyzes the data reported in this paper is available form the lead contact upon request.

ACKNOWLEDGMENTS

Funding: This work was supported by National Natural Science Foundation of China (82174033 to Y.W., 81970761 to H.R.T.).

AUTHOR CONTRIBUTIONS

Conceptualization, Q.X., H.R.T., and Y.W.; Methodology, Q.X. and Y.N.S.; Investigation, Y.P.Y. and J.H.L.; Validation and Data Curation, Y.N.S. and J.H.L.; Resources, C.H.; Writing – Original Draft, Q.X. and Y.W.; Writing – Review and Editing, Q.X.; Supervision, H.R.T.; Funding Acquisition, H.R.T. and Y.W.

DECLARATION OF INTERESTS

The authors declare that they have no known competing financial interests of personal relationships that could have appeared to influence the work reported in this paper.

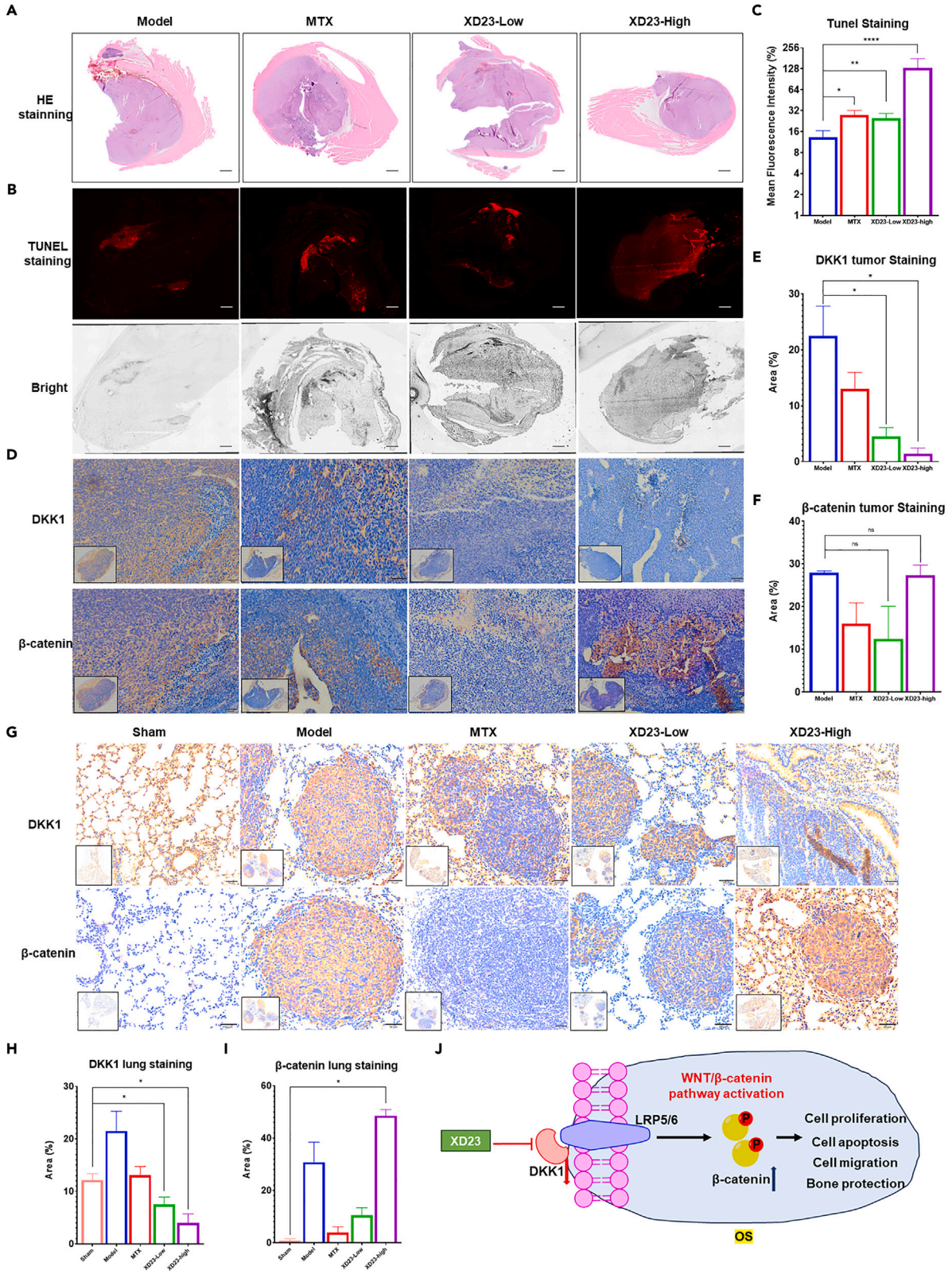
A
Model
MTX
XD23-Low
XD23-High
HE stainning
B
TUNEL staining
Bright
C
Tunel Staining
Mean Fluorescence Intensity (%)
D
DKK1
β-catenin
E
DKK1 tumor Staining
Area (%)
F
β-catenin tumor Staining
Area (%)
G
Sham
Model
MTX
XD23-Low
XD23-High
DKK1
β-catenin
H
DKK1 lung staining
Area (%)
I
β-catenin lung staining
Area (%)
J
WNT/β-catenin pathway activation
XD23
DKK1
LRP5/6
β-catenin
Cell proliferation
Cell apoptosis
Cell migration
Bone protection
OS

Figure 6. XD23's role in WNT/β-Catenin activation *in vivo*

(A) TUNEL staining of OS tissue slices from each mouse groups. Scale bars = 1 mm.

(B) TUNEL staining fluorescence intensity average.

(C) H&E staining images of OS tissue from each mouse group Scale bars = 1 mm.

(D–F) DKK1 and β-catenin IHC staining in OS tissue. Scale bars 50 μm. The relative positive area ratio of IHC staining for DKK1 (E) and β-catenin (F) in OS slices.

(G–I) IHC staining of DKK1 and β-catenin in lung slices of mice in each group. Scale bars = 50 μm. The relative positive area ratio of IHC staining for DKK1 (H) and β-catenin (I) in lung slices.

(J) XD23's mechanism of action against OS *in vivo*. *$p < 0.05$, **$p < 0.01$, ****$p < 0.0001$. ns = no significance. Data was analyzed by one-way ANOVA followed by Tukey's multiple comparisons test.

STAR★METHODS

Detailed methods are provided in the online version of this paper and include the following:

- KEY RESOURCES TABLE
- EXPERIMENTAL MODEL AND STUDY PARTICIPANT DETAILS
  - Cell lines
  - OS tumor mice model
- METHOD DETAILS
  - CCK-8 assay
  - Plate clone formation assay
  - Cell-cycle arrest analysis
  - Wounding healing assay
  - Transwell migration assay
  - Real-time quantitative PCR
  - Western Blotting
  - Micro-CT
  - Histological analysis
  - RNA-seq and data analysis
  - Plasmid transfection
- QUANTIFICATION AND STATISTICAL ANALYSIS

SUPPLEMENTAL INFORMATION

Supplemental information can be found online at https://doi.org/10.1016/j.isci.2024.110758.

Received: February 19, 2024
Revised: June 13, 2024
Accepted: August 14, 2024
Published: August 20, 2024

REFERENCES

1. Isakoff, M.S., Bielack, S.S., Meltzer, P., and Gorlick, R. (2015). Osteosarcoma: Current Treatment and a Collaborative Pathway to Success. J. Clin. Oncol. *33*, 3029–3035. https://doi.org/10.1200/jco.2014.59.4895.
2. Harrison, D.J., Geller, D.S., Gill, J.D., Lewis, V.O., and Gorlick, R. (2018). Current and future therapeutic approaches for osteosarcoma. Expert Rev. Anticancer Ther. *18*, 39–50. https://doi.org/10.1080/14737140.2018.1413939.
3. Bacci, G., Rocca, M., Salone, M., Balladelli, A., Ferrari, S., Palmerini, E., Forni, C., and Briccoli, A. (2008). High Grade Osteosarcoma of the Extremities With Lung Metastases at Presentation: Treatment With Neoadjuvant Chemotherapy and Simultaneous Resection of Primary and Metastatic Lesions. J. Surg. Oncol. *98*, 415–420. https://doi.org/10.1002/jso.21140.
4. Meyers, P.A., Schwartz, C.L., Krailo, M., Kleinerman, E.S., Betcher, D., Bernstein, M.L., Conrad, E., Ferguson, W., Gebhardt, M., Goorin, A.M., et al. (2005). Osteosarcoma: A randomized, prospective trial of the addition of ifosfamide and/or muramyl tripeptide to cisplatin, doxorubicin, and high-dose methotrexate. J. Clin. Oncol. *23*, 2004–2011. https://doi.org/10.1200/jco.2005.06.031.
5. O'Day, K., and Gorlick, R. (2009). Novel therapeutic agents for osteosarcoma. Expert Rev. Anticancer Ther. *9*, 511–523. https://doi.org/10.1586/era.09.7.
6. Ando, K., Mori, K., Corradini, N., Redini, F., and Heymann, D. (2011). Mifamurtide for the treatment of nonmetastatic osteosarcoma. Expert Opin. Pharmacother. *12*, 285–292. https://doi.org/10.1517/14656566.2011.543129.
7. Meyers, P.A., Healey, J.H., Chou, A.J., Wexler, L.H., Merola, P.R., Morris, C.D., Laquaglia, M.P., Kellick, M.G., Abramson, S.J., and Gorlick, R. (2011). Addition of Pamidronate to Chemotherapy for the Treatment of Osteosarcoma. Cancer *117*, 1736–1744. https://doi.org/10.1002/cncr.25744.
8. Smida, J., Baumhoer, D., Rosemann, M., Walch, A., Bielack, S., Poremba, C., Remberger, K., Korsching, E., Scheurlen, W., Dierkes, C., et al. (2010). Genomic Alterations and Allelic Imbalances Are Strong Prognostic Predictors in Osteosarcoma. Clin. Cancer Res. *16*, 4256–4267. https://doi.org/10.1158/1078-0432.Ccr-10-0284.
9. Grignani, G., Palmerini, E., Ferraresi, V., D'Ambrosio, L., Bertulli, R., Asaftei, S.D., Tamburini, A., Pignochino, Y., Sangiolo, D., Marchesi, E., et al. (2015). Sorafenib and everolimus for patients with unresectable high-grade osteosarcoma progressing after standard treatment: a non-randomised phase 2 clinical trial. Lancet Oncol. *16*, 98–107. https://doi.org/10.1016/s1470-2045(14)71136-2.
10. Chu, H.Y., Chen, Z., Wang, L., Zhang, Z.K., Tan, X., Liu, S., Zhang, B.T., Lu, A., Yu, Y., and Zhang, G. (2021). Dickkopf-1: A Promising Target for Cancer Immunotherapy. Front. Immunol. *12*, 658097. https://doi.org/10.3389/fimmu.2021.658097.
11. Diarra, D., Stolina, M., Polzer, K., Zwerina, J., Ominsky, M.S., Dwyer, D., Korb, A., Smolen, J., Hoffmann, M., Scheinecker, C., et al. (2007). Dickkopf-1 is a master regulator of joint remodeling. Nat. Med. *13*, 156–163. https://doi.org/10.1038/nm1538.
12. Niida, A., Hiroko, T., Kasai, M., Furukawa, Y., Nakamura, Y., Suzuki, Y., Sugano, S., and Akiyama, T. (2004). DKK1, a negative regulator of Wnt signaling, is a target of the β-catenin/TCF pathway. Oncogene *23*, 8520–8526. https://doi.org/10.1038/sj.onc.1207892.
13. Bafico, A., Liu, G., Yaniv, A., Gazit, A., and Aaronson, S.A. (2001). Novel mechanism of Wnt signalling inhibition mediated by

Dickkopf-1 interaction with LRP6/Arrow. Nat. Cell Biol. *3*, 683–686. https://doi.org/10.1038/35083081.

14. Igbinigie, E., Guo, F., Jiang, S.W., Kelley, C., and Li, J. (2019). Dkk1 involvement and its potential as a biomarker in pancreatic ductal adenocarcinoma. Clin. Chim. Acta *488*, 226–234. https://doi.org/10.1016/j.cca.2018.11.023.
15. Zhang, Y., Liang, K., Zhou, X., Zhang, X., Xu, H., Dai, H., Song, X., Yang, X., Liu, B., Shi, T., and Wei, J. (2023). Combination therapy of DKK1 inhibition and NKG2D chimeric antigen receptor T cells for the treatment of gastric cancer. Cancer Sci. *114*, 2798–2809. https://doi.org/10.1111/cas.15828.
16. Zhu, G., Song, J., Chen, W., Yuan, D., Wang, W., Chen, X., Liu, H., Su, H., and Zhu, J. (2021). Expression and Role of Dickkopf-1 (Dkk1) in Tumors: From the Cells to the Patients. Cancer Manag. Res. *13*, 659–675. https://doi.org/10.2147/cmar.S275172.
17. Goyal, L., Sirard, C., Schrag, M., Kagey, M.H., Eads, J.R., Stein, S., El-Khoueiry, A.B., Manji, G.A., Abrams, T.A., Khorana, A.A., et al. (2020). Phase I and Biomarker Study of the Wnt Pathway Modulator DKN-01 in Combination with Gemcitabine/Cisplatin in Advanced Biliary Tract Cancer. Clin. Cancer Res. *26*, 6158–6167. https://doi.org/10.1158/1078-0432.Ccr-20-1310.
18. Fulciniti, M., Tassone, P., Hideshima, T., Vallet, S., Nanjappa, P., Ettenberg, S.A., Shen, Z., Patel, N., Tai, Y.T., Chauhan, D., et al. (2009). Anti-DKK1 mAb (BHQ880) as a potential therapeutic agent for multiple myeloma. Blood *114*, 371–379. https://doi.org/10.1182/blood-2008-11-191577.
19. Noh, J.G., Jeon, H.E., So, J.S., and Chang, W.S. (2015). Effects of the Bradyrhizobium japonicum waaL(rfaL) Gene on Hydrophobicity, Motility, Stress Tolerance, and Symbiotic Relationship with Soybeans. Int. J. Mol. Sci. *16*, 16778–16791. https://doi.org/10.3390/ijms160816778.
20. González, S., Oh, D., Baclagon, E.R., Zheng, J.J., and Deng, S.X. (2019). Wnt Signaling Is Required for the Maintenance of Human Limbal Stem/Progenitor Cells In Vitro. Invest. Ophthalmol. Vis. Sci. *60*, 107–112. https://doi.org/10.1167/iovs.18-25740.
21. Dun, X., Jiang, H., Zou, J., Shi, J., Zhou, L., Zhu, R., and Hou, J. (2010). Differential expression of DKK-1 binding receptors on stromal cells and myeloma cells results in their distinct response to secreted DKK-1 in myeloma. Mol. Cancer *9*, 247. https://doi.org/10.1186/1476-4598-9-247.
22. Ke, H.Z., Richards, W.G., Li, X., and Ominsky, M.S. (2012). Sclerostin and Dickkopf-1 as Therapeutic Targets in Bone Diseases. Endocr. Rev. *33*, 747–783. https://doi.org/10.1210/er.2011-1060.
23. Lee, N., Smolarz, A.J., Olson, S., David, O., Reiser, J., Kutner, R., Daw, N.C., Prockop, D.J., Horwitz, E.M., and Gregory, C.A. (2007). A potential role for Dkk-1 in the pathogenesis of osteosarcoma predicts novel diagnostic and treatment strategies. Br. J. Cancer *97*, 1552–1559. https://doi.org/10.1038/sj.bjc.6604069.
24. Özgür, A. (2021). Investigation of anticancer activities of STA-9090 (ganetespib) as a second generation HSP90 inhibitor in Saos-2 osteosarcoma cells. J. Chemother. *33*, 554–563. https://doi.org/10.1080/1120009x.2021.1908650.
25. Goldstein, S.D., Trucco, M., Bautista Guzman, W., Hayashi, M., and Loeb, D.M. (2016). A monoclonal antibody against the Wnt signaling inhibitor dickkopf-1 inhibits osteosarcoma metastasis in a preclinical model. Oncotarget *7*, 21114–21123.
26. Shen, Y., Xie, Q., Wang, Y., Liang, J., Jiang, C., Liu, X., Wang, Y., and Hu, C. (2023). Design, synthesis and anti-osteosarcoma activity study of novel pyrido [2, 3-d] pyrimidine derivatives by inhibiting DKK1-Wnt/β-catenin pathway. Bioorg. Chem. *141*, 106848.
27. Xie, Q., Shen, Y., Meng, Y., Liang, J., Xu, J., Liang, S., Liu, X., Wang, Y., and Hu, C. (2022). Pyrido 2,3-d pyrimidine-2,4(1H,3H)-dione derivatives as RAF-MEK-ERK pathway signaling pathway blockers: Synthesis, cytotoxic activity, mechanistic investigation and structure-activity relationships. Eur. J. Med. Chem. *240*, 114579. https://doi.org/10.1016/j.ejmech.2022.114579.
28. Porter, A.G., and Jänicke, R.U. (1999). Emerging roles of caspase-3 in apoptosis. Cell Death Differ. *6*, 99–104.
29. Boulares, A.H., Yakovlev, A.G., Ivanova, V., Stoica, B.A., Wang, G., Iyer, S., and Smulson, M. (1999). Role of poly (ADP-ribose) polymerase (PARP) cleavage in apoptosis: caspase 3-resistant PARP mutant increases rates of apoptosis in transfected cells. J. Biol. Chem. *274*, 22932–22940.
30. Hitomi, J., Katayama, T., Taniguchi, M., Honda, A., Imaizumi, K., and Tohyama, M. (2004). Apoptosis induced by endoplasmic reticulum stress depends on activation of caspase-3 via caspase-12. Neurosci. Lett. *357*, 127–130.
31. Bonilla, M., Nastase, K.K., and Cunningham, K.W. (2002). Essential role of calcineurin in response to endoplasmic reticulum stress. Embo J. *21*, 2343–2353. https://doi.org/10.1093/emboj/21.10.2343.
32. Bousette, N., Chugh, S., Fong, V., Isserlin, R., Kim, K.H., Volchuk, A., Backx, P.H., Liu, P., Kislinger, T., MacLennan, D.H., et al. (2010). Constitutively active calcineurin induces cardiac endoplasmic reticulum stress and protects against apoptosis that is mediated by α-crystallin-B. Proc. Natl. Acad. Sci. USA *107*, 18481–18486. https://doi.org/10.1073/pnas.1013555107.
33. Zhao, X., Sun, S., Xu, J., Luo, Y., Xin, Y., and Wang, Y. (2018). MicroRNA-152 inhibits cell proliferation of osteosarcoma by directly targeting Wnt/β-catenin signaling pathway in a DKK1-dependent manner. Oncol. Rep. *40*, 767–774.
34. Lin, C.H., Ji, T., Chen, C.-F., and Hoang, B.H. (2014). Wnt signaling in osteosarcoma. Adv. Exp. Med. Biol. *804*, 33–45.
35. Du, X., Yang, J., Yang, D., Tian, W., and Zhu, Z. (2014). The genetic basis for inactivation of Wnt pathway in human osteosarcoma. BMC Cancer *14*, 450.
36. Cai, Y., Cai, T., and Chen, Y. (2014). Wnt pathway in osteosarcoma, from oncogenic to therapeutic. J. Cell. Biochem. *115*, 625–631.
37. Cai, Y., Mohseny, A.B., Karperien, M., Hogendoorn, P.C.W., Zhou, G., and Cleton-Jansen, A.M. (2010). Inactive Wnt/β-catenin pathway in conventional high-grade osteosarcoma. J. Pathol. *220*, 24–33.
38. Yu, F.-X., Hu, W.-J., He, B., Zheng, Y.-H., Zhang, Q.-Y., and Chen, L. (2015). Bone marrow mesenchymal stem cells promote osteosarcoma cell proliferation and invasion. World J. Surg. Oncol. *13*, 52.
39. Pan, S., Cesarek, M., Godoy, C., Co, C.M., Schindler, C., Padilla, K., Haskell, A., Barreda, H., Story, C., Poole, R., et al. (2022). Morpholino-driven blockade of Dkk-1 in osteosarcoma inhibits bone damage and tumour expansion by multiple mechanisms. Br. J. Cancer *127*, 43–55.
40. Yang, K., Xie, Q., Tang, T., Zhao, N., Liang, J., Shen, Y., Li, Z., Liu, B., Chen, J., Cheng, W., et al. (2023). Astragaloside IV as a novel CXCR4 antagonist alleviates osteoarthritis in the knee of monosodium iodoacetate-induced rats. Phytomedicine *108*, 154506. https://doi.org/10.1016/j.phymed.2022.154506.
41. Yang, K., Xie, Q., Liang, J., Shen, Y., Li, Z., Zhao, N., Wu, Y., Liu, L., Zhang, P., Hu, C., et al. (2023). Identification of Andrographolide as a novel FABP4 inhibitor for osteoarthritis treatment. Phytomedicine *118*, 154939. https://doi.org/10.1016/j.phymed.2023.154939.

STAR★METHODS

KEY RESOURCES TABLE

REAGENT or RESOURCE	SOURCE	IDENTIFIER
Antibodies		
Rabbit monoclonal to E Cadherin	Abcam	Cat#ab18203
Mouse monoclonal to E Cadherin	Abcam	Cat#ab231303
Rabbit monoclonal to N cadherin	Abcam	Cat#ab18203
Rabbit monoclonal to DKK1	Abcam	Cat#ab307367
Rabbit monoclonal to β-catenin	Abcam	Cat#ab32572
Rabbit monoclonal to β-catenin phosphor(active) S45	Abcam	Cat#ab30561
Goat Anti-Rabbit IgG H&L (HRP)	Abcam	Cat#ab6721
Goat Anti-Mouse IgG H&L (HRP)	Abcam	Cat#ab205719
Goat Anti-Rabbit Alexa Fluor® 488	Abcam	Cat#ab150077
Goat Anti-Mouse Alexa Fluor® 594	Abcam	Cat#ab150116
Rabbit monoclonal to GAPDH	Abcam	Cat#ab181602
Rabbit monoclonal to PARP	Cell Signaling Technology	Cat#9542
Rabbit polyclonal to cleaved-PARP	Cell Signaling Technology	Cat#9548
Rabbit polyclonal to caspase-12	Cell Signaling Technology	Cat#35965
Rabbit polyclonal to BAX	Cell Signaling Technology	Cat#2772
Rabbit polyclonal to Bcl-2	Cell Signaling Technology	Cat#3498
Rabbit polyclonal to caspase-3	Cell Signaling Technology	Cat#9662
Rabbit polyclonal to cleaved-caspase-3	Cell Signaling Technology	Cat#9661
Bacterial and virus strains		
Human-DKK1 plasmid	Hanyin company	N/A
Biological samples		
MICE OS tumor	This paper	N/A
MICE lung/spleen/heart/kidney/liver	This paper	N/A
Chemicals, peptides, and recombinant proteins		
XD23	Laboratory Synthesis from Shenyang Pharmaceutical University	https://www.sciencedirect.com/science/article/pii/S0223523422004810
MTX	Sigma	PHR1396
Deposited data		
Raw RNAseq data	GEO datasets	GSE262143
Original, unprocessed data	Mendeley data	https://doi.org/10.17632/kb6g5n2nnz.1
Experimental models: Cell lines		
Human osteosarcoma cell lines 143B	Stem Cell Bank of the Chinese Academy of Sciences	N/A
Human osteosarcoma cell lines MG63	Stem Cell Bank of the Chinese Academy of Sciences	N/A
Human skin fibroblasts HSF	Stem Cell Bank of the Chinese Academy of Sciences	N/A
human chondrocytes C28/I2	Stem Cell Bank of the Chinese Academy of Sciences	N/A

(*Continued on next page*)

Continued

REAGENT or RESOURCE	SOURCE	IDENTIFIER
Rat osteosarcoma cell line UMR-106	Stem Cell Bank of the Chinese Academy of Sciences	N/A
Oligonucleotides		
See Table S1 for primer sequences	N/A	N/A
Software and algorithms		
ImageJ	NIH	Version 1.52
GraphPad Prism	GraphPad	Version 9.0.0

EXPERIMENTAL MODEL AND STUDY PARTICIPANT DETAILS

Cell lines

Human osteosarcoma cell lines 143B, MG63 and Sasos2, rat osteosarcoma cell line UMR-106, human skin fibroblasts (HSF), and normal human chondrocytes (C28/I2) were procured from the Stem Cell Bank of the Chinese Academy of Sciences in Shenzhen, China. The 143B, MG63 and Sasos2 cell lines were propagated in RPMI-1640 medium (Corning, US), while HSF, C28/I2, and UMR-106 cell lines were grown in DMEM-HG medium (Corning, US). Both media were enriched with 10% fetal bovine serum (Gibco, US) and 1% penicillin-streptomycin (Gibco, US). Cultures were maintained at 37°C in a 5% CO2 atmosphere.

OS tumor mice model

In the orthotopic OS tumor model, male BALB/c nude mice (4–5 weeks old) were kept in a pathogen-free environment at SIAT and divided into 5 groups of 6: Vehicle, Sham, MTX, XD23-Low (10 mg/kg), and XD23-High (15 mg/kg). The Sham group received saline orally, while the MTX group served as a positive control with methotrexate.

UMR-106 cells were cultured, trypsinized with 0.25% trypsin, and suspended in PBS at 2 × 10^6 cells/mL. After anesthetizing with Zoletil-50 (Virbac, FR), a mouse's right hindlimb was disinfected and a syringe inserted into the tibia. Stable placement confirmed accurate needle positioning. A 30μL cell suspension was injected into the tibia of the mice, except for the Vehicle group, which received saline. Mice were monitored for body weight and tumor formation, treated after 2 weeks for 28 days, euthanized after cardiac perfusion and then dissected for organ fixation in 10% neutral formalin.

All animal handling and use was approved by Institutional Animal Care and Use Committee (IACUC) at SIAT on May 1, 2022. The registration number is SIAT-IACUC-220412-YGS-WY-A2136.

METHOD DETAILS

CCK-8 assay

Cell viability of XD23 on 143B, MG63, HSF, and C28/I2 cells was evaluated using the CCK-8 assay (DOJINDO, JP). We seeded about 5 × 10^3 cells per well in a 96-well plate. After cell adhesion, we introduced 200 μL of fresh medium with various XD23 concentrations. Post a 48h incubation, we added 10 μL of CCK-8 solution to each well and incubated for another hour. The plate was then gently shaken for around 20s, and absorbance at 450 nm was measured using a microplate reader.

Plate clone formation assay

About 8 × 10^2 143B and MG63 cells were cultured in a 6-well plate, with the medium enhanced by XD23 in concentrations ranging from 0.02 μM to 1.0 μM for 7 days post-adhesion. Afterward, the wells were PBS-rinsed and set with 4% paraformaldehyde for 15 min, followed by staining with 1% crystal violet dye solution (Solarbio, G1062#, China).

Cell-cycle arrest analysis

143B cells at 70–80% confluence in 12-well plates were treated with 0.1 μM–1.0 μM XD23 at 37°C for 48 h. Post pancreatin digestion and PBS wash, cells were fixed in 50% ethanol and stained with propidium iodide solution (Sigma, US). Flow cytometry (Beckman, 524C CytoFLEX, US) and ModFit software analyzed DNA content.

Wounding healing assay

1 × 10^6 143B cells were plated in 6-well plates with ibidi Culture-Inserts (ibidi, DE) and cultivated in serum-free medium with 0.5 μM XD23 for 24 h. Sequential images of the scratch were taken every 6 h.

Transwell migration assay

For the Transwell migration assay, a 6.5 mm Transwell with an 8.0 μm PET insert (Corning, 3464#, US) was placed in a 24-well plate and coated with a Matrigel Matrix mixture. Culture medium containing various XD23 doses was added, and 143B cells were seeded in the insert's upper chamber. After 48 h of incubation to allow migration, non-migrated cells were removed, and the rest were fixed, stained, and counted.

Real-time quantitative PCR

1 × 10^5 143B and MG63 cells were seeded in a 12-well plate at 70–80% confluence, followed by 0.5 μM XD23 treatment for 24 or 48 h. Cells were lysed with TRIZOL (Thermo Fisher, US), reverse transcribed using PrimeScript RT Master Mix (TaKaRa, RR036A#, JP), and RT-qPCR was performed on a LightCycler96 with TB Green dye (TaKaRa, RR820A#, JP), using primers listed in Table S1.

Western Blotting

Protein lysates from 143B and MG63 cells treated with XD23 for 48 h were extracted using RIPA buffer (Thermo Fisher, US), separated by 10% SDS-PAGE, and transferred to a PVDF membrane (Millipore, GER). The membrane was blocked with 2.5% skimmed milk in TBST and incubated overnight at 4°C with primary antibodies including PARP, cleaved PARP, Caspase-12, BAX, Bcl-2, Caspase-3, cleaved caspase-3, GAPDH, N-cadherin, E-cadherin, DKK1, and WNT5A.

Micro-CT

All mice limbs were positioned in a 34 mm scanning tube and imaged with a μ-CT device (Scanco Microct, Switzerland) at 18 μm resolution, using 55 kV/200μA settings[40]

Histological analysis

The internal organs were embedded in paraffin and sliced into 6-μm-thick sections. After dewaxed with xylene, rehydrated with ethanol, the sections were stained with Hematoxylin and Eosin (H&E, Beyotime, CN) as described previously.[41] Protein expression levels of DKK1 and β-catenin were evaluated by probing with corresponding antibodies on the sections.

RNA-seq and data analysis

143B cells were seeded in the 6-well plates and incubated for 48h after stimulated with 0.5 μM XD23. Then cells were lysed by TRIZOL reagent and sent to BGI Genomics institution for RNA extraction and bulk mRNA sequencing. The Raw sequencing data analysis were performed as described previously[40]

Plasmid transfection

Human-DKK1 plasmid was obtained from Hanyin company (Wuhan, CN). Lipofectamine 3000 (Invitrogen, US) was used as transfection reagent. 5 × 10^5 143B cells were seeded on 6-well plate and then performed the transfection under the manuals after 70% cells confluence. Transfection efficiency was verified by qPCR and fluorescence microscopy.

QUANTIFICATION AND STATISTICAL ANALYSIS

All experiments were conducted in triplicate, with data presented as mean ± SD from representative experiments ($n \geq 3$). Significance was denoted as ****$p < 0.0001$, ***$p < 0.001$, **$p < 0.01$, or *$p < 0.05$, analyzed using GraphPad Prism software (CA, US).